

## Three-color electrowetting display device for electronic paper

H. You and A. J. Steckl<sup>a)</sup>

Department of Electrical and Computer Engineering, Nanoelectronics Laboratory, University of Cincinnati, Cincinnati, Ohio 45221-0030, USA

(Received 31 January 2010; accepted 19 June 2010; published online 16 July 2010)

Three-color electrowetting (EW) reflective display devices have been achieved using a vertical stack structure with colored oils. Fundamental properties (interface tension and geometry) of the EW process were investigated. Arrays of  $\sim 1000$ – $2000$  pixels were constructed with pixel sizes of  $200 \times 600$  and  $300 \times 900 \mu\text{m}^2$ . Each color layer can be switched independently. Open (oil-free) area fraction of  $\sim 80\%$  in each cell is achieved at  $\sim 10$ – $12$  V. Switch-on times range from 5 to 15 ms, suitable for video content display. These characteristics demonstrate that the EW vertical structure has the potential to produce attractive video-speed color reflective electronic paper devices. © 2010 American Institute of Physics. [doi:10.1063/1.3464963]

Flat panel displays are the dominant display format in information and communication fields. For portable devices, low power consumption and the ability to work well in bright lighting conditions point to the need for reflective display technologies that do not require backlighting.<sup>1</sup> An exciting application of reflective displays is a device which emulates printed paper (electronic paper or e-paper). Several new technologies for reflective displays are being pursued.<sup>2–6</sup> Recent e-reader products use electrophoretic (EPh) displays.<sup>2</sup> However, the EPh screen image does not have the brightness of actual paper, being closer to black-on-gray than black-on-white. Furthermore, the slow switching speed<sup>2</sup> ( $\sim 1$  s) prevents the incorporation of touch commands, animation, and video.

An alternative approach for low power displays utilizes the electrowetting (EW) effect.<sup>7,8</sup> The electric field controls the wetting properties on the fluoropolymer surface, resulting in rapid manipulation of liquid on a  $\mu\text{m}$  scale.<sup>9,10</sup> EW displays can operate in both reflective<sup>7</sup> and transmissive<sup>11</sup> modes. Improvements of the hydrophobic insulator materials<sup>12,13</sup> and the working liquids have enabled EW operation at low driving voltages ( $\sim 15$  V). The EW reflective display screen has several advantages:<sup>14</sup> very thin, video rate switching speed, wide viewing angle, and low power consumption. Multicolored EW pixels composed of side-by-side monochromatic subpixels using thin film filters have been demonstrated.<sup>7</sup> However, the resolution obtainable with this approach is limited, since a full color pixel has  $3 \times$  the area of a monochromatic pixel.

In this paper, a vertical stack approach for colored EW reflective displays is demonstrated. While this approach has been previously illustrated,<sup>15</sup> no actual implementation has been reported to date. As shown in Fig. 1(a), in the vertical stack the size of the overall pixel equals that of each subpixel, significantly increasing the resolution of the display. Three-color EW display prototypes were constructed with pixels of  $300 \times 900$  and  $200 \times 600 \mu\text{m}^2$ . Each color layer can be switched independently and reversibly by applying a low voltage between the water and the bottom electrode. The EW structure consists of a dielectric-covered transparent bot-

tom electrode indium tin oxide (ITO) on the glass substrate, a hydrophobic insulator layer, a hydrophilic grid, the two fluids (water and oil), and the top electrode (needle). The hydrophobic insulator (Cytop CTL-809M, Asahi) and the underlying insulator layers ( $\text{Al}_2\text{O}_3$ ) are typically 40 nm thick and 100 nm thick, respectively. The ITO electrode is  $\sim 180$  nm. A  $\sim 8 \mu\text{m}$  high hydrophilic grid uses negative photoresist (SU-8 2010, MicroChem Corp.) to confine the oil film in each pixel. The fabrication process has been described previously.<sup>16</sup> Each EW device contains conducting (water/electrolyte) and insulating (oil) liquids. The active device area is defined by a  $25 \mu\text{m}$  wide hydrophilic grid. Multi-element ( $\sim 1000$ – $2000$ ) arrays were fabricated. The insets in Fig. 1(b) show photographs of three color arrays ( $300 \times 900 \mu\text{m}^2$  pixel size) before final assembly of the

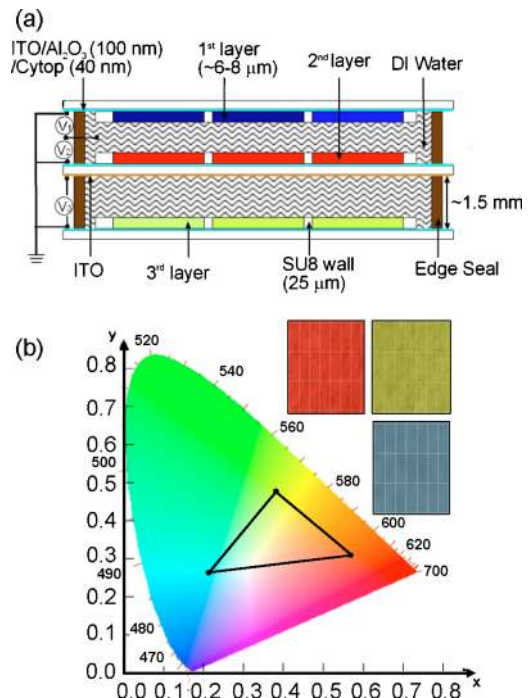


FIG. 1. (Color online) Three-color EW array using the vertical stack approach: (a) schematic diagram of device structure and (b) color coordinates of the colored oils; insets show high magnification view of  $7 \times 3$  section of the arrays.

<sup>a)</sup>Author to whom correspondence should be addressed. Electronic mail: a.steckl@uc.edu.

overall device. Individual circular devices were also fabricated.

Oils were formulated by dissolving nonpolar dyes (Keystone Co.) in dodecane: blue 98, red 164, and a yellow blend of several dyes. A mixture of the yellow and blue dyes was used to obtain the green dye. The corresponding color coordinates of 3 wt % blue, red, and green dyes in dodecane are shown in Fig. 1(b). The oil/water interfacial tension was determined by the pendant drop technique to be 15.03, 17.49, and 20.07 mN/m for green, blue, and red color oil, respectively. These values are much lower than pure dodecane/water ( $\sim 50$  mN/m). The reduction in the oil/water interface tension with the addition of dye molecules is known<sup>17</sup> to occur for concentration  $\geq 1$  wt %. This is due to dye molecules absorbing on the oil/water interface and increasing the oil surface energy and thus reducing the oil/water interface tension. The self-assembled oil dosing technique<sup>18</sup> is utilized for the array devices. Finally, the three layers are aligned and sealed under water.

In general, the contact angle (CA)  $\theta(V)$  of an oil droplet immersed in water and placed on the insulator surface depends on the electrode potential and the surface tension<sup>9</sup>

$$\cos \theta(V) = 1 - \frac{\varepsilon V^2}{2d\gamma_{OW}}, \quad (1)$$

where  $\gamma_{OW}$  is the interfacial tension between the oil and surrounding water,  $\varepsilon$  and  $d$  are the dielectric constant and the thickness of the dielectric layer. During oil contraction, the droplet did not maintain a spherical shape as it dewetted the surface, with one side being pushed against the SU-8 barrier [as seen in the photos inserted in Fig. 2(b)] while the other side was free to assume the CA dictated by the combination of interface tension and voltage. Since a circular area was not maintained, a modulation number ( $m$ ) was used to obtain an effective angle ( $\theta_{\text{eff}} = m\theta$ ) in the physical model.<sup>19</sup> Then, the pixel open area can be defined as

$$\text{OA}(V) = \left[ 1 - \frac{A_{\text{oil}}(V)}{A_{\text{pix}}} \right] = \left[ 1 - \frac{\sin^2 m\theta(V) \left\{ 1 - \frac{3}{2} \cos \alpha + \frac{1}{2} \cos^3 \alpha \right\}^{2/3}}{\sin^2 \alpha \left\{ 1 - \frac{3}{2} \cos m\theta(V) + \frac{1}{2} \cos^3 m\theta(V) \right\}^{2/3}} \right]. \quad (2)$$

$A_{\text{oil}}$  and  $A_{\text{pix}}$  denote the area occupied by oil and the overall pixel area, respectively.  $\alpha$  is the initial angle of the spherical oil cap at zero voltage<sup>19</sup> with oil in contact with the SU-8 barrier and, therefore, also depends on the oil volume.

The effect of dyes of different color on the OA fraction was investigated using the circular devices, as shown in Fig. 2. Approximately 20 and 40 nl of the colored oil were injected into the 0.9 and 1.4 mm devices resulting in average oil thickness of 7–8  $\mu\text{m}$ . The inset of Fig. 2(a) shows the OA fraction of 1.4 mm devices biased at  $-7$  V for different colored oils. The oil/water interfacial tension decreases from red to blue to green oil resulting in a monotonic increase in OA, as can be inferred from Eq. (1). The OA fraction for a blue device shown in Fig. 2(a) increases with applied voltage, reaching  $\sim 80\%$  at  $-10$  V. The two dashed lines are calculations using Eq. (2) for two  $m$  values. Good agreement between model and experiment is found for  $m=0.72$ . A value of  $m < 1$  indicates that the effective CA is smaller than one would normally obtain. This is not unexpected since the low

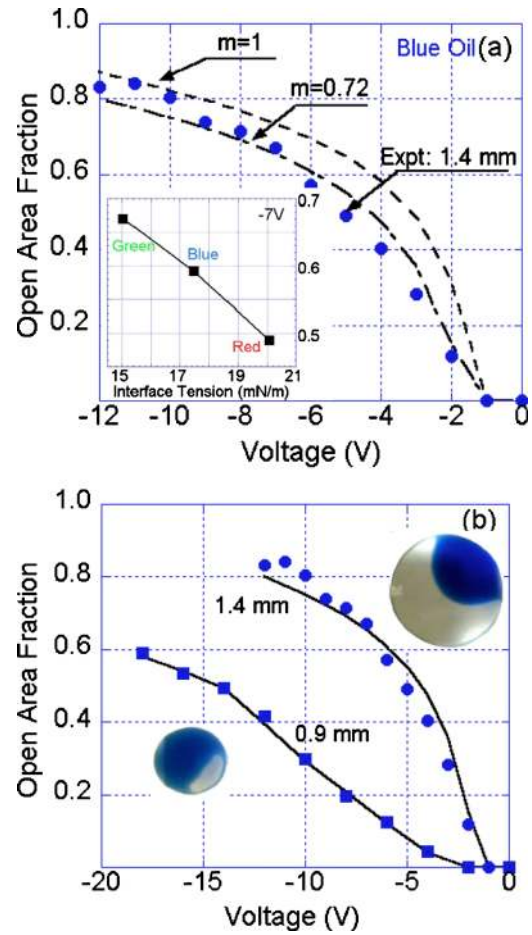


FIG. 2. (Color online) Electro-optical characteristics of circular devices as a function of applied voltage for blue oil: (a) experimental (points) and calculated OA fraction with voltage (dashed lines);  $\gamma_{OW} = 17.49$  mN/m; inset: OA fraction for dodecane with different dyes (3 wt %) at  $-7$  V. (b) OA characteristics for two cell sizes: 1.4 and 0.9 mm diameter; insets: photographs of circular devices of each diameter at  $-7$  V bias.

CA is indicative of a larger oil volume being present (than normally expected) since one side of the droplet is pinned against the SU-8 barrier. In general, a low oil/water interface tension is desirable because it can result in higher pixel OA or lower driving voltage. Decreasing the pixel size results in higher voltages to achieve the same OA fraction, as can be seen in Fig. 2(b). This is due to a sharper curvature of the oil/water interface in the smaller pixel.<sup>19</sup> This can be remedied by adjusting other device parameters, such as the SU-8 thickness and oil layer volume.

The operation of an EW stack array is illustrated in Fig. 3 where each of the three color layers is switched in turn. Figure 3(a) shows the array with all levels at zero bias, in other words with oil covering the entire pixel. In Fig. 3(b) the array is operated with  $-12$  V applied to the top blue level, resulting in  $\sim 80\%$  OA. When the top level is switched, the middle red layer is revealed. Figure 3(c) clearly shows that each red pixel is fully covered with oil. Next, the red layer is switched, revealing the bottom green layer [Fig. 3(d)]. Finally, when the bottom green layer is switched, the white background is revealed [Fig. 3(f)]. At higher voltages ( $-15$  V), up to 90% of the white substrate exposure can be reached.

The switching speed of the stacked array devices was measured using a high speed camera (TSHRMS, Fastec Im-

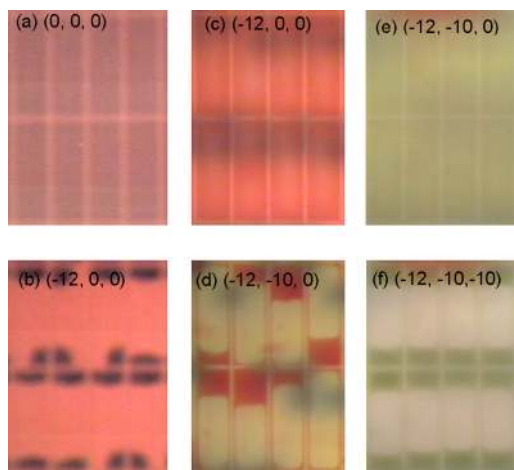


FIG. 3. (Color online) Photographs of an EW stack array ( $45 \times 21$  pixels) containing three independently switchable levels (pixel size:  $300 \times 900 \mu\text{m}^2$ ): (a) all levels in the off state, (b) top blue pixels in the on state (focused on blue level), (c) top blue pixels in the on state (focused on middle red level), (d) blue and red levels in the on state (focused on the red level), (e) blue and red levels in the on state (focused on the bottom green level), and (f) all levels in the on state (focused on green level). The numbers in each image indicate the voltage applied to the three levels.

aging Corp.) with 1000 frames per second. The response speed in a three color stack of the  $67 \times 33$  array with  $200 \times 600 \mu\text{m}^2$  pixels is shown in Fig. 4. Figure 4(a) shows the oil and water in a single pixel at 1 ms intervals in the green level under a  $-14$  V driving voltage. The OA increases with time and reaches saturation in  $\sim 10$ – $15$  ms. In the

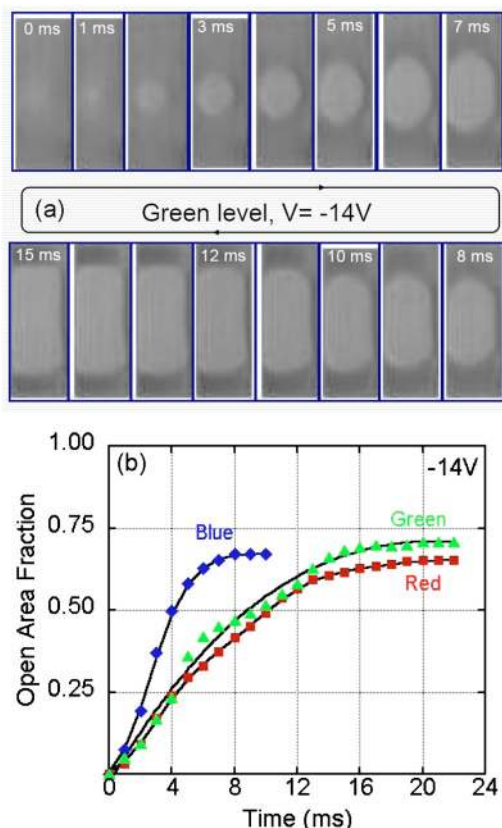


FIG. 4. (Color online) Oil motion dynamics in the  $67 \times 33$  array with  $200 \times 600 \mu\text{m}^2$  pixel size: (a) photographs of oil motion in green level at 1 ms intervals. (b) Pixel OA due to oil motion as a function of time for each color level. Average switch-on time (for 90% of saturation level) were 5.8 ms, 14.4 ms, and 13.3 ms for blue, green, and red levels, respectively.

initial oil contraction period ( $\sim 1$ – $7$  ms) the rate of oil motion is  $\sim 3$  cm/s, similar to reported values.<sup>7</sup> The switch-on time was obtained by plotting the OA percentage with time, as shown in Fig. 4(b). The switch-on times of red, blue, and green pixels (averaged over 10 pixels each) are  $13.25 \pm 2.06$ ,  $5.82 \pm 0.69$ , and  $14.39 \pm 1.75$  ms, respectively. These values are consistent with recently reported results.<sup>7,11,20</sup> The slightly faster green than red response is expected from their oil/water interface tension values. Interestingly, the blue level which has an intermediate oil/water interface tension exhibits the fastest response time. This is probably related to its location at the top of the stack, where the oil motion is evaluated with the other layers in the off state. Switch-on values of  $\sim 10$  ms were obtained for all three levels at higher voltages.

In summary, three color EW display devices using the vertical stack structure have been demonstrated. Arrays with 1000 to 2000 pixels have been fabricated. An  $\sim 80\%$  OA fraction is obtained for  $200 \times 600 \mu\text{m}^2$  pixels. The switching times of each level was  $\sim 10$  ms, significantly faster than EPh devices and in the video range. Circular structures were used to investigate fundamental properties (such as interface tension, geometry) of the EW process for different colored oils. In conclusion, the results show that EW display devices using the vertical stack structure are a very promising solution for full color reflective displays.

Support for this project by Raytheon is gratefully acknowledged. The authors appreciate many useful technical discussions on EW with members of the Nanoelectronics Laboratory and Novel Devices Laboratory at the University of Cincinnati.

- <sup>1</sup>J. Kim, C. J. Yu, D. W. Kim, and S. D. Lee, *Proc. SPIE* **5936**, 593603 (2005).
- <sup>2</sup>B. Comiskey, J. D. Albert, H. Yoshizawa, and J. Jacobson, *Nature (London)* **394**, 253 (1998).
- <sup>3</sup>M. A. Mossman, V. H. Kwong, and L. A. Whitehead, *Displays* **25**, 215 (2004).
- <sup>4</sup>H. E. A. Huitema, G. H. Gelinck, J. B. P. H. van der Putten, K. E. Kuijk, C. M. Hart, E. Cantatore, P. T. Herwig, A. J. J. M. van Breemen, and D. M. de Leeuw, *Nature (London)* **414**, 599 (2001).
- <sup>5</sup>M. Miles, E. Larson, C. Chui, M. Kothari, B. Gally, and J. Batey, *J. Soc. Inf. Disp.* **11**, 209 (2003).
- <sup>6</sup>U. Bach, D. Corr, D. Lupo, F. Pichot, and M. Ryan, *Adv. Mater. (Weinheim, Ger.)* **14**, 845 (2002).
- <sup>7</sup>R. A. Hayes and B. J. Feenstra, *Nature (London)* **425**, 383 (2003).
- <sup>8</sup>J. Heikenfeld, K. Zhou, E. Kreitz, B. Raj, S. Yang, B. Sun, A. Milarcik, L. Clapp, and R. Schwartz, *Nat. Photonics* **3**, 292 (2009).
- <sup>9</sup>F. Mugelet and J. C. Baret, *J. Phys.: Condens. Matter* **17**, R705 (2005).
- <sup>10</sup>C. Quilliet and B. Berge, *Curr. Opin. Colloid Interface Sci.* **6**, 34 (2001).
- <sup>11</sup>J. Heikenfeld and A. J. Steckl, *Appl. Phys. Lett.* **86**, 151121 (2005).
- <sup>12</sup>H. Moon, S. K. Cho, R. L. Garrell, and C. J. Kim, *J. Appl. Phys.* **92**, 4080 (2002).
- <sup>13</sup>E. Seyrat and R. A. Hayes, *J. Appl. Phys.* **90**, 1383 (2001).
- <sup>14</sup>R. Shama, D. Andelman, B. Berge, and R. Hayes, *Soft Matter* **4**, 38 (2008).
- <sup>15</sup>White Paper from Liquavista, <http://www.liquavista.com/downloads/default.aspx>.
- <sup>16</sup>D. Y. Kim and A. J. Steckl, *Langmuir* **26**, 9474 (2010).
- <sup>17</sup>T. Roques-Carmes, S. Palmier, R. A. Hayes, and L. J. M. Schlangen, *Colloids Surf., A* **267**, 56 (2005).
- <sup>18</sup>B. Sun, K. Zhou, Y. Lao, J. Heikenfeld, and W. Cheng, *Appl. Phys. Lett.* **91**, 011106 (2007).
- <sup>19</sup>T. Roques-Carmes, R. A. Hayes, and L. J. M. Schlangen, *J. Appl. Phys.* **96**, 6267 (2004).
- <sup>20</sup>T. Roques-Carmes, R. A. Hayes, B. J. Feenstra, and L. J. M. Schlangen, *J. Appl. Phys.* **95**, 4389 (2004).